ISBN: 978-3-95450-223-3 ISSN: 2673-7000 doi:10.18429/JACoW-NAPAC2019-TUYBB6

BEAM DYNAMICS IN A HIGH-GRADIENT RF STREAK CAMERA*

A. Landa, V.A. Dolgashev, F. Toufexis†, SLAC, Menlo Park, CA, USA

Abstract

Traditionally, time-resolved experiments in storage ring synchrotron light sources and free-electron lasers are performed with short x-ray pulses with time duration smaller than the time resolution of the phenomenon under study. Typically, storage-ring synchrotron light sources produce x-ray pulses on the order of tens of picoseconds. Newer diffraction limited storage rings produce even longer pulses. We propose to use a high-gradient RF streak camera for time-resolved experiments in storage-ring synchrotron light sources with potential for sub-100 fs resolution. In this work we present a detailed analysis of the effects of the initial time and energy spread of the photo-emitted electrons on the time resolution, as well as a start-to-end beam dynamics simulation in an S-Band system.

INTRODUCTION

The motivation for this work is twofold: to enable measurement of x-ray pulse structure in Free-Electron Lasers (FELs) and sub-picosecond time-resolved experiments in storage-ring synchrotron light sources. There is currently no practical method of directly instrumenting the time structure of the x-ray pulse in an FEL; this measurement is performed indirectly by streaking the electron beam after the undulators with an rf deflector [1–3]. Storage-ring synchrotron light sources typically produce x-ray pulses on the order of tens of picoseconds that allow for time-resolved experiments with sub-nanosecond resolution. Newer diffraction limited storage rings produce even longer pulse lengths. An ultrafast streak camera would enable sub-picosecond intensity-based time-resolved experiments with long x-ray pulses. It is also possible that diffraction-based experiments could be performed using the 2D movie reconstruction techniques discussed in [4–7].

Streak cameras are instruments for measuring the variation in a pulse of light's intensity with time. The time structure of the incident light pulse is encoded onto an electron beam through a photocathode. The photo-electrons are accelerated and then streaked producing a 2D image on a screen, from which the intensity versus time of the light pulse can be inferred. Streak cameras have been used in particle accelerators for a variety of instrumentation tasks including bunch length measurements, longitudinal instability measurements, characterization of FEL performance, and synchronization in pump-probe experiments [8]. They have also been used for plasma diagnostics [9–11]. The 2D image of visible light streak cameras was used to create a 2D movie of the propagation of a light pulse [4–6] and a similar concept has been studied for an X-ray streak camera [7].

* This project was funded by U.S. Department of Energy under Contract No. DE-AC02-76SF00515.
† ftouf@slac.stanford.edu

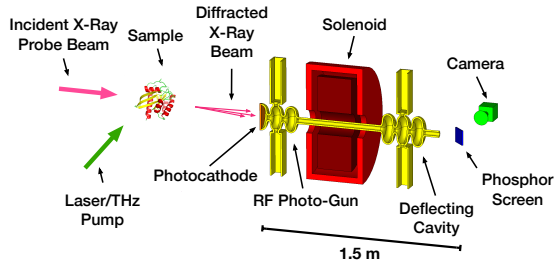

Figure 1: High-gradient rf streak camera concept, adapted from Toufexis *et al.* [25].

The typical time resolution of X-ray streak cameras is on the order of a few ps, primarily dominated by the bunch lengthening due to the initial energy spread of the photo-electons and low accelerating field on the photocathode. With photocathode fields on the order of 10 kV mm^{-1}, single-shot sub-picosecond streak cameras have been demonstrated with 600 fs Full Width Half Max (FWHM), 350 fs rise time, and 50 fs timing jitter [10, 12–14]. In accumulation mode, time resolution down to 233 fs was achieved [15, 16]. However, all these experiments used Ultraviolet (UV) light instead of an X-ray beam. It was shown in simulation that using low-power accelerating RF fields may improve the resolution down to 100 fs [17, 18]. Experiments using THz radiation [19] and laser light [20, 21] have shown resolution of 10 fs and 100 as, respectively. RF deflectors have been used to capture ultrafast processes in a single shot in ultrafast electron diffraction with 150 fs FWHM temporal resolution [22–24].

In this work we propose the use of a high-gradient RF photo-injector and RF deflector as an ultra-high-resolution X-ray streak camera operating in either single-shot or accumulation mode. This concept is shown in Fig. 1. Our initial work was reported in [25]. Here we show a detailed analysis of the effects on the time resolution of the initial time and energy spread of the photo-emitted electrons both analytically and numerically, using the beam dynamics code ASTRA [26]. Finally, we show a start-to-end beam dynamics simulation of the system; the S-Band photo-gun and deflector are discussed in detail in [25].

DEFINITION OF RESOLUTION

Typically the FWHM of one pulse is used as a measure of the time resolution in streak cameras [10, 12–14]. In this work we define the X time resolution Δt^X as the spacing between two photon pulses at the cathode that results in $\frac{N_V}{N_{LP}} = X$, as shown in Fig. 2. This approach is a similar to what is used in optics [27]. We will report the FWHM, the 50 %, and the 80 % resolution below.

If we have two photon pulses with some overlap in time then the combined distribution will have two peaks and a val-

ISBN: 978-3-95450-223-3 ISSN: 2673-7000 doi:10.18429/JACoW-NAPAC2019-TUYBB6

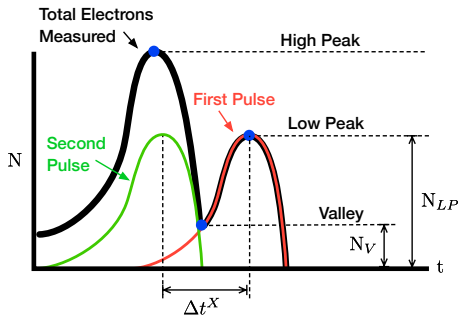

Figure 2: Time resolution calculation overview.

ley in-between, as shown in Fig. 2. Due to this overlap, both the amplitude and position of the pulses will be distorted. Typically, the electron pulses generated in the gun are neither symmetric or Gaussian. Furthermore, the propagation through the system may change the pulse tails. As a result, when two pulses are added, the situation in Fig. 2 arises; there is a low peak corresponding to the first pulse and a high peak corresponding to the second pulse that overlaps with the the tail of the first.

X-RAY PHOTO-EMISSION MODEL

Here we discuss the photo-emission model we use in our simulations. As discussed in [28], the secondary electron initial kinetic energy δE distribution can be modeled with the following Probability Density Function (PDF):

$$f_{\delta E}(E_K; W) = 6W^2 \frac{E_K}{(E_K + W)^4}, \quad (1)$$

where W is the work function of the material. The direction of the momentum corresponding to this initial kinetic energy is uniformly distributed in the azimuth ϕ and as $\cos\theta$ in the elevation angle θ, where θ defined from the normal vector to the cathode surface. We assume the time delay δt between the incident photon and emitted secondary electron is distributed according to a similar PDF:

$$f_{\delta t}(t; T_d) = 6T_d^2 \frac{t}{(t + T_d)^4}, \quad (2)$$

where T_d is the parameter controlling the time spread of the secondary electrons. Figure 3 shows plots of the PDF of these distributions for different values W from [29] and T_d. Note that we have revised our model from [25] to capture the transverse energy spread and be on par with the literature [28]. Additionally, in [25] we have incorrectly exported the initial energy distribution in ASTRA, thus underestimating the effect of the initial energy spread and emittance it is associated with.

EFFECT OF INITIAL TIME SPREAD

To isolate the effect of the initial time spread of the photo-electrons on the resolution from the other effects we simulated the generation of pairs of photon pulses with zero transverse and longitudinal dimensions, $\sigma_r = 0\,\mu\text{m}$ and

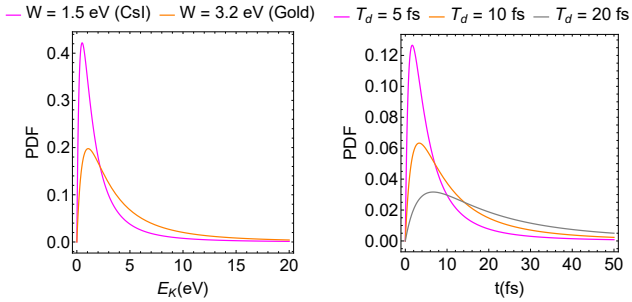

(a) Initial energy distribution PDF from Fig. 14 of [29].

(b) Delay of electron emission PDF.

Figure 3: X-ray photo-emission model.

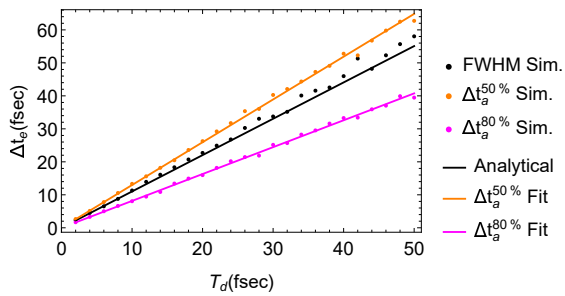

Figure 4: Time resolution only due to initial time spread versus T_d.

$\sigma_t = 0\,\text{fs}$, and applied the photo-emission model to get the distribution of the photo-electrons in time. We used 50,000 particles per pulse and calculated the time resolution right after the cathode from the longitudinal phase space of the electrons. The results are shown in Fig. 4. The 50 % and 80 % resolution data fits are given by

$$\Delta t_{e,n}^{50\,\%} = 1.30 \cdot T_d, \quad \Delta t_{e,n}^{80\,\%} = 0.81 \cdot T_d. \quad (3)$$

Also shown in Fig. 4 is a comparison with the analytical expression

$$\Delta t_{e,a} = 1.1 \cdot T_d, \quad (4)$$

the FWHM of equation (2). This shows that the initial time spread distribution imposes a fundamental limit on the resolution that needs to be quantified experimentally.

EFFECT OF INITIAL ENERGY SPREAD AND CATHODE SURFACE FIELD

To isolate the effect of the initial energy spread of the photo-electrons due to the cathode work function W and the cathode surface field E_{acc} on the resolution from the other effects we simulated the generation of pairs of photon pulses with zero transverse and longitudinal dimensions, $\sigma_r = 0\,\mu\text{m}$ and $\sigma_t = 0\,\text{fs}$, and applied the photo-emission model with varying work function W but zero time spread $T_d = 0\,\text{fs}$ to get the distribution of the photo-electrons in time. We tracked those electrons with ASTRA through the gun for various gun gradients E_{acc} at on-crest gun phase. We used 50,000 particles per pulse and calculated the time

ISBN: 978-3-95450-223-3 ISSN: 2673-7000 doi:10.18429/JACoW-NAPAC2019-TUYBB6

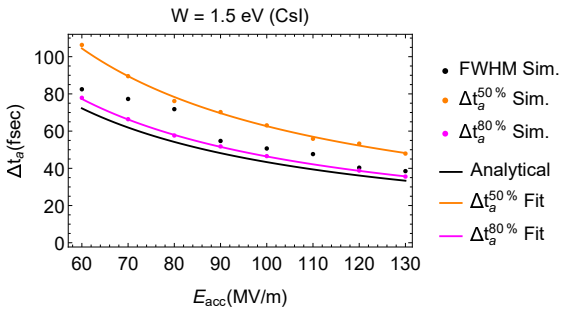

(a) CsI $W = 1.5$ eV.

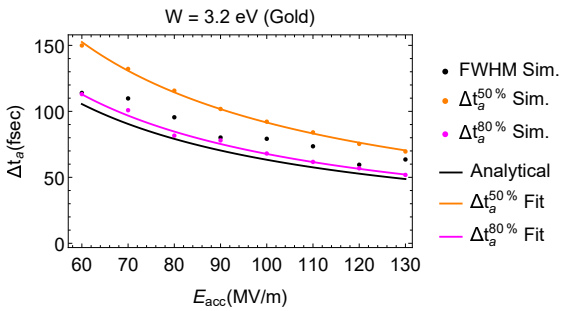

(b) Gold $W = 3.2$ eV.

Figure 5: Time resolution only due to initial energy spread of photo-electrons versus the cathode surface field for different cathode materials [29].

resolution at the exit of the gun from the longitudinal phase space of the electrons. The results are shown in Fig. 5. The lower the work function W and the higher the accelerating gradient E_{acc}, the higher the resolution. The 50 % and 80 % resolution data fits are given by

$$\Delta t_{a,n}^{50\,\%} = \frac{5.1\sqrt{W}}{E_{acc}}\,(\mathrm{ps}), \quad \Delta t_{a,n}^{80\,\%} = \frac{3.8\sqrt{W}}{E_{acc}}\,(\mathrm{ps}). \qquad (5)$$

Also shown in Fig. 5 is a comparison with the published analytical expression [10, 12, 15, 18, 25]

$$\Delta t_{a,a} \approx \frac{1}{E_{acc}}\sqrt{\frac{2m_e\delta E}{q_e}} \approx \frac{3.5\sqrt{W}}{E_{acc}}\,(\mathrm{ps}), \qquad (6)$$

where δE is the FWHM of the electron energy in eV, and E_{acc} is the accelerating field on the photocathode in kV mm^{-1}.

START-TO-END SIMULATION

We performed a start-to-end beam dynamics simulation to quantify the resolution of the overall system. The parameters of the photo-emission model were $T_d = 10$ fs and $W = 3.2$ eV (gold), the cathode surface field was $E_{acc} = 120\,\mathrm{MV\,m^{-1}}$, the rms spot size was $\sigma_r = 5\,\mu$m, the photon pulse length was zero, and the peak deflecting voltage was 3.5 MV. We used 100,000 particles per pulse and calculated the time resolution at a screen position at 1.5 m downstream of the cathode. The FWHM was 128 fs,

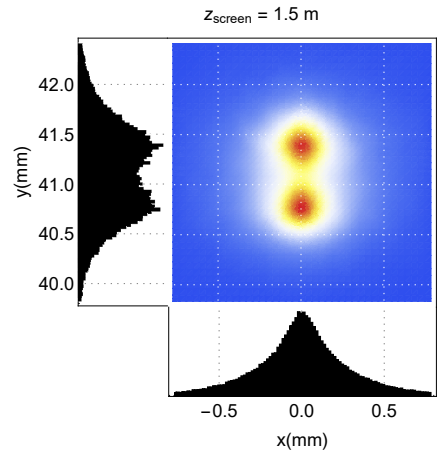

Figure 6: Transverse beam distribution imaged on a screen from two zero-length pulses spaced 136 fs apart. The parameters of the photo-emission model were $T_d = 10$ fs and $W = 3.2$ eV (gold), the cathode surface field was $E_{acc} = 120\,\mathrm{MV\,m^{-1}}$, the rms spot size was $\sigma_r = 5\,\mu$m, and the peak deflecting voltage was 3.5 MV.

$\Delta t^{50\,\%} = 204$ fs, and $\Delta t^{80\,\%} = 136$ fs. Figure 6 shows the transverse beam distribution imaged on the screen from two zero-length pulses spaced 136 fs apart, the 80 % resolution; the two pulses are clearly distinguished. The distance between the pulses on the screen can be converted to time at the cathode by multiplying by 2.2 ps cm^{-1}. With $E_{acc} = 130\,\mathrm{MV\,m^{-1}}$ and using CsI $W = 1.5$ eV instead of gold we get a FWHM of 96 fs, $\Delta t^{50\,\%} = 145$ fs, and $\Delta t^{80\,\%} = 95$ fs. However, it is unclear if CsI is compatible with high-gradient RF fields.

CONCLUSION

We have presented a new concept for an ultra-fast X-ray streak camera. In this system, the X-ray beam is focused on the photocathode of a high-gradient radio-frequency cavity that accelerates the photo-emitted electrons to a few MeV while preserving their time structure. The accelerated electron beam is streaked by a radio-frequency deflector and imaged on a phosphor screen. We presented a detailed analysis of the effects on the time resolution of the initial time and energy spread of the photo-emitted electrons both analytically and numerically. The initial time spread distribution imposes a fundamental limit on the resolution that needs to be quantified experimentally. We further presented a start-to-end simulation of the overall system. Given the published data and the analysis we performed here, it appears that near-100 fs resolution is possible using a high-gradient S-Band system. Higher resolution is also possible using higher cathode surface field and higher frequency, e.g. X-Band.

ACKNOWLEDGMENTS

The authors wish to thank Georgi Dakovski, Yiping Feng, Ingolf Lindau, Piero Pianetta, Thomas Rabedeau, and Dimosthenis Sokaras for fruitful conversions.

ISBN: 978-3-95450-223-3 ISSN: 2673-7000 doi:10.18429/JACoW-NAPAC2019-TUYBB6

REFERENCES

[1] P. Emma, J. Frisch, and P. Krejcik, "A Transverse RF deflecting structure for bunch length and phase space diagnostics," Tech. Rep., Aug. 2000.

[2] R. Akre, L. Bentson, P. Emma, and P. Krejcik, "A Transverse RF deflecting structure for bunch length and phase space diagnostics," Tech. Rep., Jun. 2001.

[3] V. A. Dolgashev *et al.*, "Design and application of multimegawatt X-band deflectors for femtosecond electron beam diagnostics," *Phys. Rev. ST Accel. Beams*, vol. 17, no. 10, p. 102801, Oct. 2014.

[4] L. Gao *et al.*, "Single-shot compressed ultrafast photography at one hundred billion frames per second," *Nature*, vol. 516, no. 7529, pp. 74–77, Dec. 2014.

[5] J. Liang *et al.*, "Encrypted Three-dimensional Dynamic Imaging using Snapshot Time-of-flight Compressed Ultrafast Photography," *Scientific Reports*, vol. 5, no. 1, p. 15504, Oct. 2015.

[6] ——, "Single-shot real-time video recording of a photonic Mach cone induced by a scattered light pulse," *Science Advances*, vol. 3, no. 1, p. e1601814, 2017.

[7] D. S. Badali and R. J. Dwayne Miller, "Robust reconstruction of time-resolved diffraction from ultrafast streak cameras," *Structural Dynamics*, vol. 4, no. 5, p. 054302, 2017.

[8] K. Scheidt, "Review of Streak Cameras for Accelerators: Features, Applications and Results," in *Proc. 7th European Particle Accelerator Conf. (EPAC'00)*, Vienna, Austria, Jun. 2000, paper WEYF202, pp. 182–186.

[9] H. Shiraga, M. Nakasuji, M. Heya, and N. Miyanaga, "Two-dimensional sampling-image x-ray streak camera for ultrafast imaging of inertial confinement fusion plasmas," *Review of Scientific Instruments*, vol. 70, no. 1, pp. 620–623, 1999.

[10] P. Gallant *et al.*, "Characterization of a subpicosecond x-ray streak camera for ultrashort laser-produced plasmas experiments," *Review of Scientific Instruments*, vol. 71, no. 10, pp. 3627–3633, 2000.

[11] A. G. MacPhee *et al.*, "Improving the off-axis spatial resolution and dynamic range of the NIF X-ray streak cameras (invited)," *Review of Scientific Instruments*, vol. 87, no. 11, p. 11E202, 2016.

[12] Z. Chang *et al.*, "Demonstration of a sub-picosecond x-ray streak camera," *Applied Physics Letters*, vol. 69, no. 1, pp. 133–135, 1996.

[13] J. Liu *et al.*, "An accumulative x-ray streak camera with sub-600-fs temporal resolution and 50-fs timing jitter," *Applied Physics Letters*, vol. 82, no. 20, pp. 3553–3555, 2003.

[14] J. Feng *et al.*, "A grazing incidence x-ray streak camera for ultrafast, single-shot measurements," *Applied Physics Letters*, vol. 96, no. 13, p. 134102, 2010.

[15] M. M. Shakya and Z. Chang, "Achieving 280fs resolution with a streak camera by reducing the deflection dispersion," *Applied Physics Letters*, vol. 87, no. 4, p. 041103, 2005.

[16] J. Feng *et al.*, "An x-ray streak camera with high spatio-temporal resolution," *Applied Physics Letters*, vol. 91, no. 13, p. 134102, 2007.

[17] A. Tron and I. Merinov, "Method of bunch radiation photochronography with 10 femtosecond and less resolution," *International Journal of Modern Physics A*, vol. 22, no. 23, pp. 4187–4197, 2007.

[18] J. Qiang, J. M. Byrd, J. Feng, and G. Huang, "X-ray streak camera temporal resolution improvement using a longitudinal time-dependent field," *Nuclear Instruments and Methods in Physics Research Section A: Accelerators, Spectrometers, Detectors and Associated Equipment*, vol. 598, no. 2, pp. 465–469, 2009.

[19] U. Frühling *et al.*, "Single-shot terahertz-field-driven X-ray streak camera," *Nature Photonics*, vol. 3, no. 9, pp. 523–528, Sep. 2009.

[20] J. Itatani *et al.*, "Attosecond Streak Camera," *Phys. Rev. Lett.*, vol. 88, p. 173903, Apr. 2002.

[21] M. Uiberacker *et al.*, "Attosecond metrology with controlled light waveforms," *Laser Phys*, vol. 15, pp. 195–204, 2005.

[22] P. Musumeci *et al.*, "Capturing ultrafast structural evolutions with a single pulse of MeV electrons: Radio frequency streak camera based electron diffraction," *Journal of Applied Physics*, vol. 108, no. 11, p. 114513, 2010.

[23] G. H. Kassier *et al.*, "A compact streak camera for 150 fs time resolved measurement of bright pulses in ultrafast electron diffraction," *Review of Scientific Instruments*, vol. 81, no. 10, p. 105103, 2010.

[24] C. Lee, G. Kassier, and R. J. D. Miller, "Optical fiber-driven low energy electron gun for ultrafast streak diffraction," *Applied Physics Letters*, vol. 113, no. 13, p. 133502, 2018.

[25] F. Toufexis and V. A. Dolgashev, "Sub-Picosecond X-Ray Streak Camera using High-Gradient RF Cavities," in *10th Int. Particle Accelerator Conf. (IPAC'19), Melbourne, Australia, May 2019*, pp. 4256–4259.

[26] K. Floettmann, *ASTRA*, Deutsches Elektronen-Synchrotron, Hamburg, Germany. [Online]. Available: www.desy.de/~mpyflo/Astra_manual/Astra-Manual_V3.1.pdf

[27] L. R. F.R.S., "Xxxi. investigations in optics, with special reference to the spectroscope," *The London, Edinburgh, and Dublin Philosophical Magazine and Journal of Science*, vol. 8, no. 49, pp. 261–274, 1879. [Online]. Available: doi:10.1080/14786447908639684

[28] B. L. Henke, J. A. Smith, and D. T. Attwood, "0.1–10-keV x-ray-induced electron emissions from solids—Models and secondary electron measurements," *Journal of Applied Physics*, vol. 48, no. 5, pp. 1852–1866, 1977.

[29] B. L. Henke, J. P. Knauer, and K. Premaratne, "The characterization of x-ray photocathodes in the 0.1–10-keV photon energy region," *Journal of Applied Physics*, vol. 52, no. 3, pp. 1509–1520, 1981.